Implementation of the Motion Controller for an Omni Mobile Robot Using the Trajectory Linearization Control

Vu Hoan Bui[1,2], Chi Tuan Duong[1,2], Trong Nhan Nguyen[1,2], The Cuong Le[1,2], Xuan Quang Ngo[1,2], Duy Khang Luong[1,2], Nhat An Ho[1,2], Huy Vu Phung[1,2], Tri Manh Vo[1,2], and Ha Quang Thinh Ngo[1,2](✉)

[1] Department of Mechatronics Engineering, Faculty of Mechanical Engineering, Ho Chi Minh City University of Technology (HCMUT), 268 Ly Thuong Kiet Street, District 10, Ho Chi Minh City 700000, Vietnam
nhqthinh@hcmut.edu.vn

[2] Vietnam National University Ho Chi Minh City, Linh Trung Ward, Thu Duc District, Ho Chi Minh City 700000, Vietnam

Abstract. This study introduces the design and modeling of nonlinear controller based on the omni-wheel for mobile robot. Via/Through the dynamics characteristics, the control scheme of Trajectory Linearization Control (TLC) is developed. Furthermore, the proposed controller is simulated in order to verify the effectiveness and feasibility. From the simulation results, the proposed controller achieves superior performance such 20% better tracking error, 10% faster transient period and converge to finite time.

Keywords: Omni-robot · Mobile robot · Trajectory linearization control · Simulation

1 Introduction

The main object of this research is an omni-directional robot which is a kind of holonomic mobile platform. The flexibility, maneuverability and highly practical application capabilities cause why many scientists have researched about this robot [1].

In our investigation, omni-directional robot has 03 orthogonal wheels that are fixed at each vertex of an even triangle and controlled by the DC servo motors and the main MCU (micro-controller unit). Also, an embedded computer is utilized to calculate the inverse kinetic and receive directives from main PC (personal computer) through LAN (local area network). Besides, the position of the object is determined by a roof camera. Base on this location, PC could manipulate the mission for tracking trajectory to follow the path that is generated by the process of trajectory planning.

With the above researches, most of previous studies have been targeted on the dynamic analysis and mechanical design. However, the dynamical model and highly precise control to track path/trajectory have not been studied deeply. In many topics of omni-directional dynamic models, the ideal servo motor is used to drive the motors as

P. Cong Vinh and N. Huu Nhan (Eds.): ICTCC 2021, LNICST 408, pp. 51–66, 2021.
https://doi.org/10.1007/978-3-030-92942-8_5

well as the responses of motor can adapts to the desired command without error [7]. In the real condition, the dynamical constraints of servo motor could significantly affect on the robot motion. The dynamic model and control strategies of the omni-directional mobile robot is developed and discussed in [2] and [3]. Nevertheless, these controllers are based on the linear control method while the robot dynamics are nonlinear. Additionally, the feedback gain of the controllers has to be tuned to achieve system stability for different trajectories. This is also solved by fuzzy and adaptive method in [3]. But in a dynamic environment such as sportive applications, it is really difficult to predetermine the trajectory and adjust the feedback gain in real-time to combine both stability and transient response of the robot control system. Besides, [8] introduces an adaptive control method unknowing the center of gravity (C.o.G). However, in our scope, C.o.G could be determined via mechanical design software and considered unchanged during working time. Friction and slip are also ignored despite being mentioned at [9] and handled by an adaptive backstepping control method. Additionally, the feedback gain of the controllers has to be tuned to achieve system stability for different trajectories.

In the dynamic environment such sportive applications, it is really difficult to predetermine the trajectory and adjust the feedback gain in real time to combine both stability and transient response of the robot control system. To achieve better performance, it is desired that the controller for tracking trajectory could follow any given feasible path. In this research, TLC scheme on omni-directional mobile robot which combines nonlinear inverse kinetic duty of linearly time-varying eigen structure, is investigated [4]. The nonlinear tracking and decoupling control by trajectory linearization can be handled as the perfect gain-scheduling controller that designed at every point on the trajectory. Therefore, the TLC provides robust stability and excellent performance along the trajectory without interpolation of controller gains.

In Sect. 2: The kinematics, dynamics of the robot and the DC motor of omni-directional mobile robot model is presented.

In Sect. 3: Create controller for the robot using TLC method.

In Sect. 4: Simulation test result.

In Sect. 5: Conclusion & Plan.

2 The Mathematical Model of Omni-Directional Mobile Robot

Initially, in order to design a controller for robot, the descriptions of robot motion are essential to be indicated with some assumptions as below.

Assumption 1: Since the electrical time constant of the motor is too small, the wheels roll on a flat without slipping and the friction force is simplified to be represented by a viscous damping coefficient.

Assumption 2: The unmodeled dynamics will be compensated by the feedback controller which is based on this simplified model in the next section.

2.1 Coordinates and Symbols

Let the mobile robot be rigid moving on the workspace. It is assumed that the world coordinate system $O_wX_wY_wZ_w$ is fixed on the ground, and the local coordinate system $O_mX_mY_mZ_m$ is fixed on the C.o.G (Center of Gravity) of the mobile robot as Fig. 1.

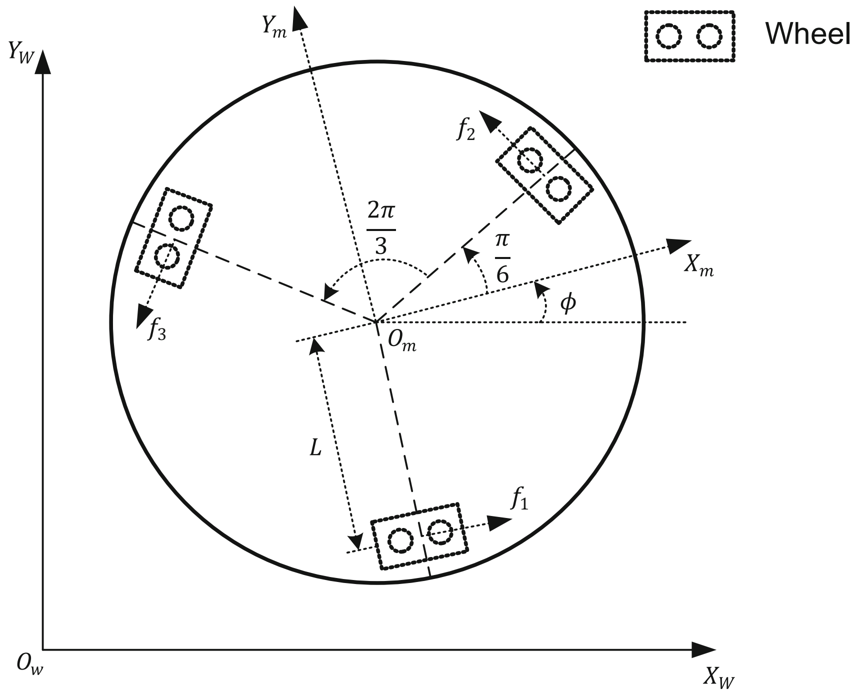

Fig. 1. Model of an omni-directional mobile robot

The following mathematical notations are utilized to depict this system:

- L: the distance between driving motor and C.o.G of the robot
- m: the weight of robot
- I: the moment inertia of robot
- R: the radius of driving wheels
- n: gear ratio between motor and wheel
- $w = [w_1 \quad w_2 \quad w_3]^T$: the angular velocities of the 1st, 2nd and 3rd wheel respectively
- $w_m = [w_{m1} \quad w_{m2} \quad w_{m3}]^T$: the angular velocities of the 1st, 2nd and 3rd motor correspondingly
- $v_T = [v_{w1} \quad v_{w2} \quad v_{w3}]^T$: the tangential velocity of the 1st, 2nd and 3rd wheel respectively

Then, the location of robot is expressed in the world coordinate as following

- ${}^{W}r = \begin{bmatrix} {}^{W}x & {}^{W}y & {}^{W}\phi \end{bmatrix}^{T}$: the position of the robot's C.o.G
- ${}^{W}v = \begin{bmatrix} {}^{W}v_x & {}^{W}v_y & {}^{W}v_\phi \end{bmatrix}^{T}$: the robot's velocities consisting of linear velocities and angular velocity

Moreover, some system parameters are illustrated in the local coordinate which attached to the body of robot.

- ${}^{m}r = [{}^{m}x \quad {}^{m}y \quad {}^{m}\phi]^{T}$: the position of the robot's C.o.G
- ϕ: the rotational angle between the X_W and the X_m axis
- ${}^{m}v = [{}^{m}v_x \quad {}^{m}v_y \quad {}^{m}v_\phi]^{T}$: the robot's velocities including linear velocities and angular velocity
- $f = [f_1 \quad f_2 \quad f_3]^{T}$: the traction forces of the wheels.

2.2 Robot Kinematics

The relationship between tangential velocity at each wheel and velocity of the robot based on the Fig. 2.

$$\begin{bmatrix} v_{w1} \\ v_{w2} \\ v_{w3} \end{bmatrix} = \begin{bmatrix} 1 & 0 & L \\ -\frac{1}{2} & \frac{\sqrt{3}}{2} & L \\ -\frac{1}{2} & -\frac{\sqrt{3}}{2} & L \end{bmatrix} \begin{bmatrix} {}^{m}v_x \\ {}^{m}v_x \\ {}^{m}v_\phi \end{bmatrix} \tag{1}$$

We have,

$$w = \frac{v_T}{R} \tag{2}$$

$$w_m = nw \tag{3}$$

Since the driving motor is directly attached to the omni wheel, from Eq. (1), (2) and (3) the relationship between the rotational velocities of the motors and its velocities is determined as

$$\begin{bmatrix} w_{m1} \\ w_{m2} \\ w_{m3} \end{bmatrix} = B^{T} \frac{n}{R} \begin{bmatrix} {}^{m}v_x \\ {}^{m}v_y \\ {}^{m}v_\phi \end{bmatrix} \tag{4}$$

where, $B = \begin{bmatrix} 1 & -\frac{1}{2} & -\frac{1}{2} \\ 0 & \frac{\sqrt{3}}{2} & -\frac{\sqrt{3}}{2} \\ L & L & L \end{bmatrix}$

As a result, with the matrix transformation ${}^{W}R_m$ from the local coordinate to the world coordinate, the kinematic equation of the system could be re-written as

$${}^{W}v = {}^{W}R_m {}^{m}v = {}^{W}R_m \frac{R}{n} \left(B^{T}\right)^{-1} w_m \tag{5}$$

Where, ${}^{W}R_m = \begin{bmatrix} \cos\phi & -\sin\phi & 0 \\ \sin\phi & \cos\phi & 0 \\ 0 & 0 & 1 \end{bmatrix}$.

2.3 Robot Dynamic

The acceleration of the point with respect to the world coordinate system $O_wX_wY_wZ_w$

$$\begin{aligned} \vec{a}_{P/O_W} = \vec{a}_{O_m/O_W} + \left(\vec{a}_{P/O_m}\right)_{O_mX_mY_mZ_m} + 2\vec{w}_{O_W} \times \left(\vec{v}_{P/O_m}\right)_{O_mX_mY_mZ_m} \\ + \dot{\vec{w}} \times \vec{r}_{P/O_m} + \vec{w}_{O_W} \times \vec{v}_{P/O_m} \end{aligned} \tag{6}$$

Where,

- $\vec{a}_{P/O_W}$: the acceleration of point P, the point on the robot, with respect to the frame O_W;
- $\vec{a}_{O_m/O_W}$: the acceleration of the frame O_m with respect to the frame O_W; $\left(\vec{a}_{P/O_m}\right)_{O_mX_mY_mZ_m}$: the acceleration of point P with respect to the frame O_m, $\left(\vec{a}_{P/O_m}\right)_{O_mX_mY_mZ_m} = 0$;
- $2\vec{w}_{O_W} \times \left(\vec{v}_{P/O_m}\right)_{O_mX_mY_mZ_m}$: the Coriolis acceleration, $2\vec{w}_{O_W} \times \left(\vec{v}_{P/O_m}\right)_{O_mX_mY_mZ_m} = 0$;
- $\dot{\vec{w}} \times \vec{r}_{P/O_m}$: the Euler acceleration, $\dot{\vec{w}} \times \vec{r}_{P/O_m} = 0$;
- $\vec{w}_{O_W} \times \vec{v}_{P/O_m}$: the centripetal acceleration;
- $\vec{w} = \dot{\phi}\vec{k}$;
- $\vec{v}_{P/O_m} = {}^{m}v_x\vec{i} + {}^{m}v_y\vec{j}$;
- $\vec{w} \times \vec{v}_{P/Om} = r\vec{k} \times \left({}^{m}v_x\vec{i} + {}^{m}v_y\vec{j}\right) = r^{m}v_x\vec{j} - r^{m}v_y\vec{i}$;

So, rewrite the Eq. (6)

$$\vec{a}_{P/O_W} = \vec{a}_{O_m/O_W} + r^{m}v_x\vec{j} - r^{m}v_y\vec{i} \tag{7}$$

Applying Newton's law

$$\sum \vec{F} = m\vec{a}_{P/O_W} \tag{8}$$

Projecting the Eq. (8) onto O_mX_m, O_mY_m, O_mZ_m axis respectively

$$F_X = m\left({}^{m}\dot{v}_x - r^{m}v_y\right) \tag{9}$$

$$F_Y = m\left({}^{m}\dot{v}_y + r^{m}v_x\right) \tag{10}$$

$$T = I\,{}^{m}\dot{v}_{\phi} \tag{11}$$

Obtaining the dynamical performance of the omni mobile robot based on the Eq. (9), (10) and (11), we have

$$\begin{bmatrix} {}^{m}\dot{v}_x \\ {}^{m}\dot{v}_y \\ {}^{m}\dot{v}_{\phi} \end{bmatrix} = \begin{bmatrix} {}^{m}v_{\phi}{}^{m}v_y \\ -{}^{m}v_{\phi}{}^{m}v_x \\ 0 \end{bmatrix} + HB\begin{bmatrix} f_1 \\ f_2 \\ f_3 \end{bmatrix} \tag{12}$$

Where, $H = \begin{bmatrix} \frac{1}{m} & 0 & 0 \\ 0 & \frac{1}{m} & 0 \\ 0 & 0 & \frac{1}{I} \end{bmatrix}$

In [5], the dynamic characteristics of each DC motor can be demonstrated as

$$L_a\frac{di_a}{dt} + R_a i_a + k_b w_m = u \tag{13}$$

$$J_m\,\dot{w}_m + D_m w_m + \frac{Rf}{n} = k_t i_a \tag{14}$$

Where,

- u is the applied armature voltage;
- i_a is the armature current;
- L_a is the armature inductance;
- R_a is the armature resistance;
- k_b is the back emf constant;
- k_t is the motor torque constant;
- J_m is the equivalent inertia at the armature including both the armature inertia and the load inertia referred to the armature such as gear train, wheel, etc.;
- D_m is the equivalent viscous damping at the armature including both the armature viscous damping and the load viscous damping referred to the armature such as gear train, wheel, etc.

Since the electrical time constant is negligible comparing to the mechanical time constant, we could achieve

$$\frac{di_a}{dt} = 0 \tag{15}$$

Substituting the Eq. (15) into the Eq. (14), we have

$$i_a = \frac{1}{R_a}(u - k_b w_m) \tag{16}$$

From the Eqs. (4), (12), (14) and (16), we get the dynamics equation of the system in the body frame in respect to the supplied voltage to the motor $u = \begin{bmatrix} u_1 & u_2 & u_3 \end{bmatrix}^T$

$$G\begin{bmatrix} {}^m\dot{v}_x \\ {}^m\dot{v}_y \\ {}^m\dot{v}_\phi \end{bmatrix} = \begin{bmatrix} {}^m v_\phi {}^m v_y \\ -{}^m v_\phi {}^m v_x \\ 0 \end{bmatrix} - HBB^T \frac{n^2}{R^2}\left(D_m + \frac{k_t k_b}{R_a}\right)\begin{bmatrix} {}^m v_x \\ {}^m v_y \\ {}^m v_\phi \end{bmatrix} + HB\frac{n}{R}\frac{k_t}{R_a}\begin{bmatrix} u_1 \\ u_2 \\ u_3 \end{bmatrix} \tag{17}$$

Where, $G = I + HBB^T J_m \frac{n^2}{R^2}$.

3 Controller Design

In the previous works [6], three speed controllers of the driving motor were independently installed in omni-directional mobile robot. Like almost omni-directional robots, the signal control of each motor controller is established by the inverse dynamic of the robot model. In fact, most of mobile robots could not track the desired following path because the open-loop controller exists inevitable errors. The errors should be eliminated or reduced to zero.

Designing a controller design bases on TLC, which is showed in this section. TLC has been proven to be a successful technique in nonlinear decoupling, disturbance reduction and following path [2, 4, 7]. TLC is considered as the ideal gain-scheduling controller to track point on the path. The controller consists of two loop parts. The inside loop is the hardware constraints of controller to obey the control command from the outside loop. The outside loop modifies the position of robot based on the information of the vision system. The first part is the feedforward controller, which is formulated to automatically tuning the parameters of a system by mean of dynamic inversion. The second part is a feedback controller, which forces the robot to return to the reference trajectory.

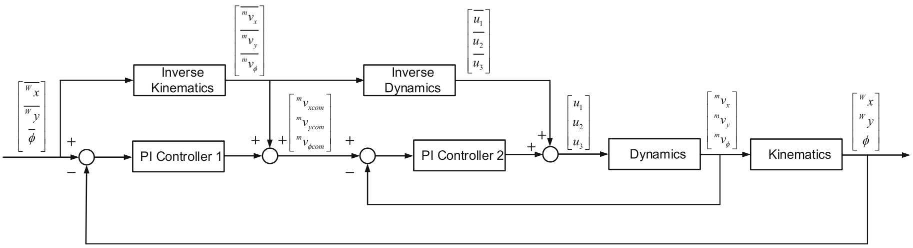

Fig. 2. The structure of proposed controller using TLC for the omni mobile robot

3.1 Outer Loop Control

Through the kinematic Eq. (5), based on the desired trajectory $\left[\overline{{}^{W}x}(t) \quad \overline{{}^{W}y}(t) \quad \overline{\phi}\,(t)\right]^{T}$, the nominal velocity of the system might be calculated as

$$\begin{bmatrix} \dot{\overline{{}^{m}x}} \\ \dot{\overline{{}^{m}y}} \\ \dot{\overline{\phi}} \end{bmatrix} = \begin{bmatrix} \cos\overline{\phi} & \sin\overline{\phi} & 0 \\ -\sin\overline{\phi} & \cos\overline{\phi} & 0 \\ 0 & 0 & 1 \end{bmatrix} \begin{bmatrix} \dot{\overline{{}^{W}x}} \\ \dot{\overline{{}^{W}y}} \\ \dot{\overline{\phi}} \end{bmatrix} \tag{18}$$

The linearization of the function about the equilibrium point is then given by:

$$\begin{aligned} \dot{x}_i &= f_i(x_1, x_2, \ldots, x_n, u_1, u_2, \ldots, u_m) \\ &\approx \sum_{j=1}^{n} \frac{\partial f_i}{\partial x_j}\bigg|_{x_j=\overline{x_j}} \left(x_j - \overline{x_j}\right) + \sum_{j=1}^{m} \frac{\partial f_i}{\partial u_j}\bigg|_{u_j=\overline{u_j}} \left(u_j - \overline{u_j}\right) \end{aligned} \tag{19}$$

Where,

- $x_1, x_2, \ldots, x_n, u_1, u_2, \ldots, u_m$: the states and inputs;
- $\overline{x_1}, \overline{x_2}, \ldots, \overline{x_n}, \overline{u_1}, \overline{u_2}, \ldots, \overline{u_m}$: the equilibrium points;

From the Eq. (18) and the Eq. (19), we have

$$\dot{x_1} = {}^{W}\dot{x} = \cos\phi\,{}^{m}v_x - \sin\phi\,{}^{m}v_y = f_1\left({}^{W}x, {}^{W}y, \phi, {}^{m}v_x, {}^{m}v_y, \dot{\phi}\right) \tag{20}$$

$$\dot{x_2} = {}^{W}\dot{y} = \cos\phi\,{}^{m}v_x - \sin\phi\,{}^{m}v_y = f_2\left({}^{W}x, {}^{W}y, \phi, {}^{m}v_x, {}^{m}v_y, \dot{\phi}\right) \tag{21}$$

$$\dot{x_3} = \dot{\phi} = f_3\left({}^{W}x, {}^{W}y, \phi, {}^{m}v_x, {}^{m}v_y, \dot{\phi}\right) \tag{22}$$

Furthermore, we define several mathematical notations for tracking purpose

$$\begin{bmatrix} e_x \\ e_y \\ e_\phi \end{bmatrix} = \begin{bmatrix} {}^{W}x \\ {}^{W}y \\ \phi \end{bmatrix} - \begin{bmatrix} \overline{{}^{W}x} \\ \overline{{}^{W}x} \\ \overline{\phi} \end{bmatrix} \tag{23}$$

$$\begin{bmatrix} \delta^{m}v_x \\ \delta^{m}v_y \\ \delta^{m}v_\phi \end{bmatrix} = \begin{bmatrix} {}^{m}v_{xcom} \\ {}^{m}v_{ycom} \\ {}^{m}v_{\phi com} \end{bmatrix} - \begin{bmatrix} \overline{{}^{m}v_x} \\ \overline{{}^{m}v_y} \\ \overline{{}^{m}v_\phi} \end{bmatrix} \tag{24}$$

Linearizing Eq. (20), (21), (22) about the nominal trajectory $\left[\overline{{}^{W}x}(t) \quad \overline{{}^{W}y}(t) \quad \overline{\phi}\,(t)\right]^{T}$ and $\left[\overline{{}^{m}v_x} \quad \overline{{}^{m}v_y} \quad \overline{{}^{m}v_\phi}\right]^{T}$ based on the Eq. (19), we have

$$\dot{e_x} = \left(-\sin\overline{\phi}\,{}^{m}v_x - \cos\overline{\phi}\,{}^{m}v_y\right)e_\phi + \cos\phi\,\delta^{m}v_x - \sin\phi\,\delta^{m}v_y \tag{25}$$

$$\dot{e_y} = \left(\cos\overline{\phi}^m v_x - \sin\overline{\phi}^m v_y\right)e_\phi + \sin\phi\delta^m v_x + \cos\phi\delta^m v_y \tag{26}$$

$$\dot{e_\phi} = \delta^m v_\phi \tag{27}$$

From Eq. (25), (26) and (27), we have

$$\begin{bmatrix} \dot{e_x} \\ \dot{e_y} \\ \dot{e_\phi} \end{bmatrix} = A_1 \begin{bmatrix} e_x \\ e_y \\ e_\phi \end{bmatrix} + B_1 \begin{bmatrix} \delta^m v_x \\ \delta^m v_y \\ \delta^m v_\phi \end{bmatrix} \tag{28}$$

where,

$$A_1 = \begin{bmatrix} 0 & 0 & -\sin\overline{\phi}^m v_x - \cos\overline{\phi}^m v_y \\ 0 & 0 & \cos\overline{\phi}^m v_x - \sin\overline{\phi}^m v_y \\ 0 & 0 & 0 \end{bmatrix}; \quad B_1 = \begin{bmatrix} \cos(\phi) & -\sin(\phi) & 0 \\ \sin(\phi) & \cos(\phi) & 0 \\ 0 & 0 & 1 \end{bmatrix}$$

Later, the PI (Proportional-Integral) controller is designed to stabilize the system performance

$$\begin{bmatrix} \delta^m v_x \\ \delta^m v_y \\ \delta^m v_\phi \end{bmatrix} = -K_{P1} \begin{bmatrix} e_x \\ e_y \\ e_\phi \end{bmatrix} - K_{I1} \begin{bmatrix} \int e_x(t)dt \\ \int e_y(t)dt \\ \int e_\phi(t)dt \end{bmatrix} \tag{29}$$

From the Eq. (28) and (29), we get

$$\dot{x_o} = A_{clo} x_o \tag{30}$$

Where,

$$x_o = \begin{bmatrix} \int e_x(t)dt \\ \int e_y(t)dt \\ \int e_\phi(t)dt \\ e_x(t) \\ e_y(t) \\ e_\phi(t) \end{bmatrix}; \qquad \begin{matrix} A_{clo} = \begin{bmatrix} O_3 & I_3 \\ -B_1 K_{I1} & A_1 - B_1 K_{P1} \end{bmatrix}; \\ O_3 \text{ is the } 3 \times 3 \text{ zero matrix;} \\ I_3 \text{ is the } 3 \times 3 \text{ identity matrix;} \end{matrix} \tag{31}$$

Design K_{P1} and K_{I1} to achieve the desired closed-loop tracking error dynamics

$$A_{clo} = \begin{bmatrix} O_3 & I_3 \\ diag[-a_{111} \quad -a_{121} \quad -a_{131}] & diag[-a_{112} \quad -a_{122} \quad -a_{132}] \end{bmatrix} \tag{32}$$

Where $a_{1j1} > 0$, $a_{1j2} > 0, j = 1, 2, 3$ are the coefficients of the desired closed-loop characteristic polynomial of each channel.

Based on the desired response and tracking error, we choose the suitable poles, and then define the coefficients of the desired closed-loop characteristic polynomial.

From Eq. (31) and Eq. (32), we get the gain K_{P1} and K_{I1} of the controller

$$\begin{aligned} K_{I1} &= -B_1^{-1} diag[-a_{111} \quad -a_{121} \quad -a_{131}] \\ K_{P1} &= B_1^{-1}(A_1 - diag[-a_{112} \quad -a_{122} \quad -a_{132}]) \end{aligned} \tag{33}$$

The tracking command for the inner loop is given by

$$\begin{bmatrix} {}^m v_{xcom} \\ {}^m v_{ycom} \\ {}^m v_{\phi com} \end{bmatrix} = \begin{bmatrix} \overline{{}^m v_x} \\ \overline{{}^m v_y} \\ \overline{{}^m v_\phi} \end{bmatrix} + \begin{bmatrix} \delta^m v_x \\ \delta^m v_y \\ \delta^m v_\phi \end{bmatrix} \tag{34}$$

3.2 Inner Loop Control

By using the kinematic Eq. (17), we can get the nominal values of control voltages for the driving motors owing to the nominal velocities of the system $\begin{bmatrix} \overline{{}^m v_x} & \overline{{}^m v_y} & \overline{{}^m v_\phi} \end{bmatrix}^T$

$$\begin{aligned} \begin{bmatrix} \overline{u_1} \\ \overline{u_2} \\ \overline{u_3} \end{bmatrix} &= \left(HB\frac{n}{R}\frac{k_t}{R_a}\right)^{-1} G \begin{bmatrix} \dot{\overline{{}^m v_x}} \\ \dot{\overline{{}^m v_y}} \\ \dot{\overline{{}^m v_\phi}} \end{bmatrix} - \left(HB\frac{n}{R}\frac{k_t}{R_a}\right)^{-1} \begin{bmatrix} \overline{{}^m v_\phi {}^m v_y} \\ -\overline{{}^m v_\phi {}^m v_x} \\ 0 \end{bmatrix} \\ &+ B^T \frac{n}{R}\frac{R_a}{k_t}\left(D_m + \frac{k_t k_b}{R_a}\right) \begin{bmatrix} \overline{{}^m v_x} \\ \overline{{}^m v_y} \\ \overline{{}^m v_\phi} \end{bmatrix} \end{aligned} \tag{35}$$

Additionally, the below quantities are mathematically defined

$$\begin{bmatrix} e_{{}^m v_x} \\ e_{{}^m v_y} \\ e_{{}^m v_\phi} \end{bmatrix} = \begin{bmatrix} {}^m v_x \\ {}^m v_y \\ {}^m v_\phi \end{bmatrix} - \begin{bmatrix} {}^m v_{xcom} \\ {}^m v_{ycom} \\ {}^m v_{\phi com} \end{bmatrix} \tag{36}$$

$$\begin{bmatrix} \delta u_1 \\ \delta u_2 \\ \delta u_3 \end{bmatrix} = \begin{bmatrix} u_1 \\ u_2 \\ u_3 \end{bmatrix} - \begin{bmatrix} \overline{u_1} \\ \overline{u_2} \\ \overline{u_3} \end{bmatrix} \tag{37}$$

Linearizing along the nominal trajectories $\begin{bmatrix} \overline{{}^m v_x} & \overline{{}^m v_y} & \overline{{}^m v_\phi} \end{bmatrix}^T$ and $\begin{bmatrix} \overline{u_1} & \overline{u_2} & \overline{u_3} \end{bmatrix}^T$ based on the Eq. (19) in the similar procedure to outer loop control, so we attain the tracking error dynamics of inner loop

$$\begin{bmatrix} \dot{e}_{^m v_x} \\ \dot{e}_{^m v_y} \\ \dot{e}_{^m v_\phi} \end{bmatrix} = A_2 \begin{bmatrix} e_{^m v_x} \\ e_{^m v_y} \\ e_{^m v_\phi} \end{bmatrix} + B_2 \begin{bmatrix} \delta u_1 \\ \delta u_2 \\ \delta u_3 \end{bmatrix} \tag{38}$$

Where,

$$A_2 = G^{-1} \begin{bmatrix} 0 & \overline{^m v_\phi} & \overline{^m v_y} \\ -\overline{^m v_\phi} & 0 & \overline{^m v_x} \\ 0 & 0 & 0 \end{bmatrix} - G^{-1} HBB^T \frac{n^2}{R^2} \left(D_m + \frac{k_t k_b}{R_a} \right);$$
$$B_2 = G^{-1} HB \frac{k_t}{R_a} \frac{n}{R};$$

Similarly, we design a PI controller in order to stabilize the tracking error:

$$\begin{bmatrix} \delta u_1 \\ \delta u_2 \\ \delta u_3 \end{bmatrix} = -K_{P2} \begin{bmatrix} e_{^m v_x} \\ e_{^m v_y} \\ e_{^m v_\phi} \end{bmatrix} - K_{I2} \begin{bmatrix} \int e_{^m v_x}(t)dt \\ \int e_{^m v_y}(t)dt \\ \int e_{^m v_\phi}(t)dt \end{bmatrix} \tag{39}$$

From the Eq. (38) and (39), we get:

$$\dot{x}_i = A_{cli} x_i \tag{40}$$

Where,

$$x_i = \begin{bmatrix} \int e_{^m v_x}(t)dt \\ \int e_{^m v_y}(t)dt \\ \int e_{^m v_\phi}(t)dt \\ e_{^m v_x}(t) \\ e_{^m v_y}(t) \\ e_{^m v_\phi}(t) \end{bmatrix}; \qquad A_{cli} = \begin{bmatrix} O_3 & I_3 \\ -B_2 K_{I2} & A_2 - B_2 K_{P2} \end{bmatrix}; \tag{41}$$

O_3 is the 3×3 zero matrix;
I_3 is the 3×3 identity matrix;

Design K_{P2} and K_{I2} to achieve the desired closed-loop tracking error dynamics

$$A_{cli} = \begin{bmatrix} O_3 & I_3 \\ diag[-a_{211} \quad -a_{221} \quad -a_{231}] & diag[-a_{212} \quad -a_{222} \quad -a_{232}] \end{bmatrix} \tag{42}$$

Where $a_{2j1} > 0$, $a_{2j2} > 0$, $j = 1, 2, 3$ are the coefficients of the desired closed-loop characteristic polynomial of each channel.

Based on the desired response and tracking error, we choose the suitable poles, and then define the coefficients of the desired closed-loop characteristic polynomial.

From Eq. (41) and Eq. (42), we get the gain K_{P2} and K_{I2} of the controller

$$\begin{aligned} K_{I2} &= -B_2^{-1} diag[-a_{211} \quad -a_{221} \quad -a_{231}] \\ K_{P2} &= B_2^{-1}(A_2 - diag[-a_{212} \quad -a_{222} \quad -a_{232}]) \end{aligned} \tag{43}$$

Finally, the control input voltage to the motors is computed as

$$\begin{bmatrix} u_1 \\ u_2 \\ u_3 \end{bmatrix} = \begin{bmatrix} \delta u_1 \\ \delta u_2 \\ \delta u_3 \end{bmatrix} + \begin{bmatrix} \overline{u_1} \\ \overline{u_2} \\ \overline{u_3} \end{bmatrix} \tag{44}$$

4 Results of Study

In the simulation, we test the omni robot in two different trajectories: (i) a set-point trajectory, (ii) a circular trajectory. We can use the same control gains to follow these two trajectories.

The omni-directional robot has three dimensions of freedom. It can drive in translation and rotation independently. In the simulation, robot can be controlled to track translation and rotation trajectories at the same time.

4.1 Location Control

The initial position of robot is [0 0 0] and robot is move to stop at [0.05 0.05 π/4] from initial position. The simulation result is shown in Fig. 3.

4.2 Circular Trajectory

In the simulation, the mobile robot was controlled to accelerate from the initial position [0 0.5 0] and circularly move with the increasing angular speed from 0.05 rad/s to 1 rad/s. The center of the circular route was at [0 0] on Oxy coordinate and the robot body was maintained on the tangential direction of circle. The simulation outcomes are presented in Fig. 4 and Fig. 5. According to Fig. 4, the azimuth tracking error Ψ is displayed on the resolution of 0.001 radians, and the tracking error x and y in the resolution of 0.001 m.

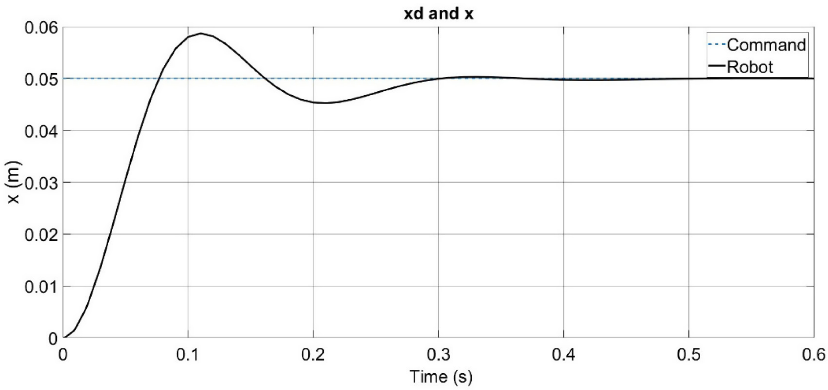

(a)

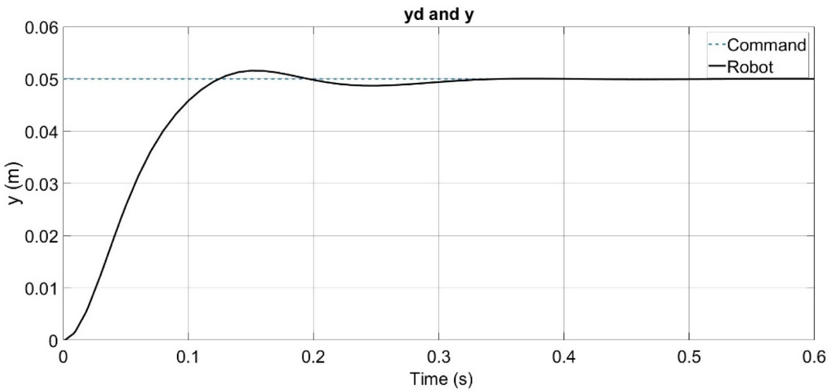

(b)

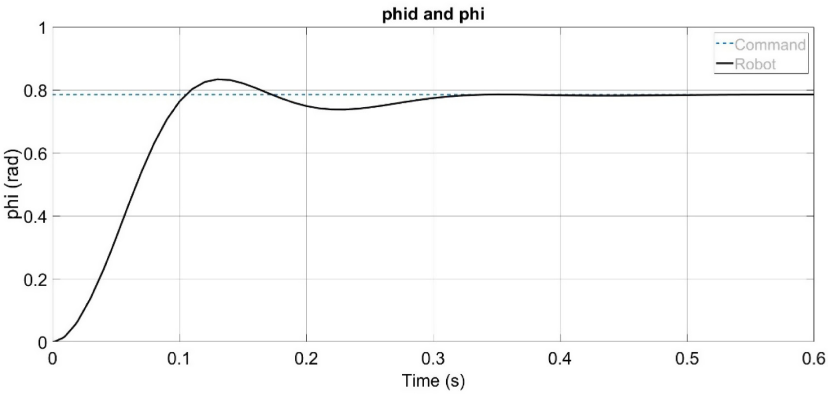

(c)

Fig. 3. Position control (a), (b) and (c) tracking result on x axis, y axis and rotational axis respectively

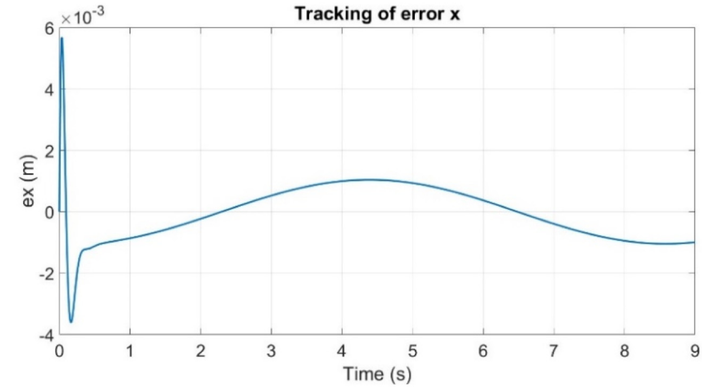

(a)

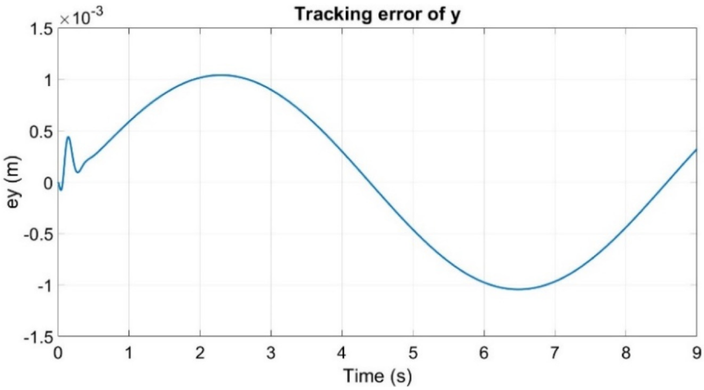

(b)

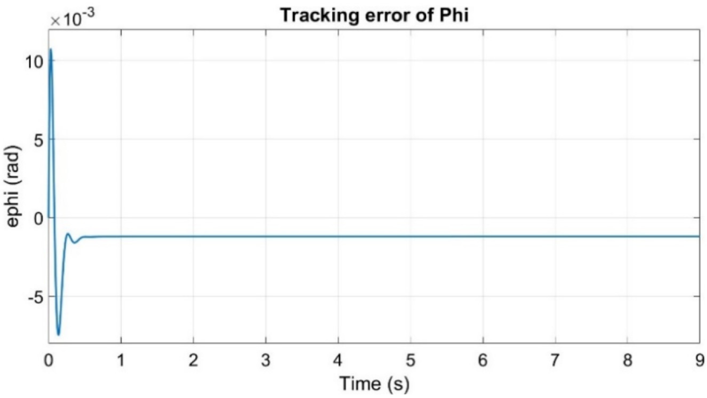

(c)

Fig. 4. (a), (b) and (c) Tracking errors of circular trajectory

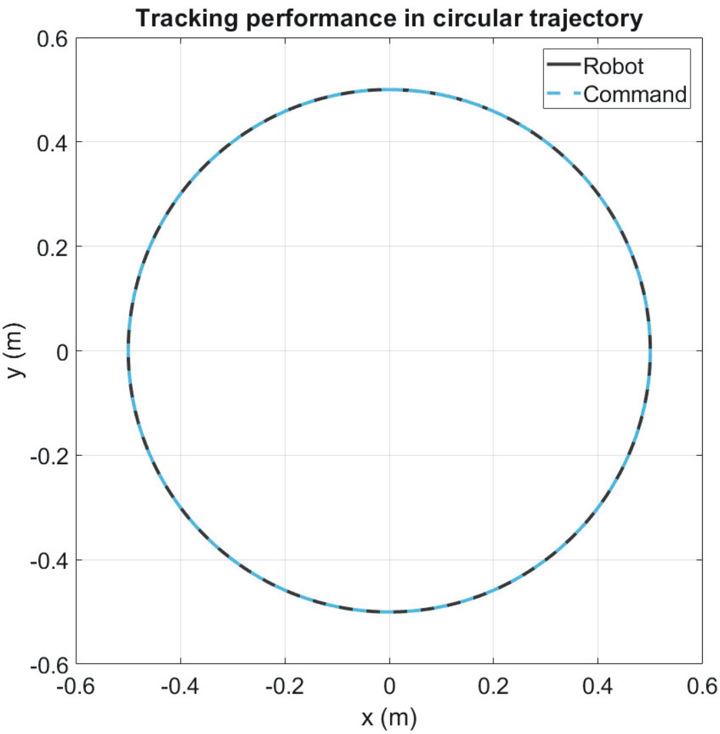

Fig. 5. Circular trajectory plot of omni robot

5 Conclusions

This article presented the equations of motion for an omni robot via dynamics, kinematics, and motor actuator to simulate the hardware platform. Based on these formulas, a nonlinear controller was implemented to design by TLC method. The simulation results showed that the robot can track trajectory with relative accuracy and the settling time is reasonable. Using this linearization approach, the controller gains could be tuned easily.

From the simulation results, it can be seen the proposed scheme for omni robot is robust, feasible and efficient. Future work is a must. Although our method is theoretically simulated, it is necessary to verify in a real hardware. Alternatively, a visual equipment with artificial intelligence or machine learning might be integrated into robot platform.

Acknowledgments. We acknowledge the support of time and facilities from Ho Chi Minh City University of Technology (HCMUT), VNU-HCM for this study.

References

1. Pin, F.G., Killough, S.M.: A new family of omnidirectional and holonomic wheeled platforms for mobile robots. IEEE Trans. Robot. Autom. **10**(4), 480–489 (1994)
2. Watanabe, K., Shiraishi, Y., Tzafestas, S.G., Tang, J., Fukuda, T.: Feedback control of an omnidirectional autonomous platform for mobile service robots. J. Intell. Rob. Syst. **22**(3), 315–330 (1998). https://doi.org/10.1023/A:1008048307352
3. Watanabe, K.: Control of an omnidirectional mobile robot. In: 1998 Second International Conference on Knowledge-Based Intelligent Electronic Systems. Proceedings KES 1998 (Cat. No. 98EX111), vol. 1, pp. 51–60, April 1998
4. Zhu, J.J., Banker, B.D., Hall, C.E.: X-33 ascent flight controller design by trajectory linearization-a singular perturbational approach. In: Proceedings of AIAA Guidance, Navigation, and Control Conference, August 2000
5. Nguyen, T.P., Nguyen, H., Phan, V.H., Ngo, H.Q.T.: Modeling and practical implementation of motion controller for stable movement in a robotic solar panel dust-removal system. Energy Sources Part A Recovery Utilization Environ. Eff. 1–22 (2021)
6. Zheng, Z.W., Huo, W.: Trajectory tracking control for a stratospheric airship. Control Decis. **26**(10), 1479–1484 (2011)
7. Choi, J.S., Kim, B.K.: Near minimum-time direct voltage control algorithms for wheeled mobile robots with current and voltage constraints. Robotica **19**(1), 29 (2001)
8. Huang, J.-T., Van Hung, T., Tseng, M.-L.: Smooth switching robust adaptive control for omnidirectional mobile robots. IEEE Trans. Control Syst. Technol. **23**(5), 1986–1993 (2015)
9. Huang, H.-C., Tsai, C.-C.: Adaptive trajectory tracking and stabilization for omnidirectional mobile robot with dynamic effect and uncertainties. IFAC Proc. Vol. **41**(2), 5383–5388 (2008)